more than 15 cm^{-1} compared to the gas-phase value (*17*). Thus, the observed matrix band of C_{13} should be in a frequency region between 1780 and 1795 cm^{-1}.

From the data observed so far, it appears for neutral and anionic carbon clusters from C_{10} to C_{20} that linear and cyclic isomers coexist in laser-vaporized graphite, despite theoretical predictions that the cyclic rings should be considerably more stable [≥20 kcal/mol (*7–9*)] than the linear chains. At the high temperature (approximately 4000 K) of graphite vaporization, entropy strongly favors the formation of linear over cyclic isomers because of the higher density of states that results from the low bending frequencies of the linear structures. Therefore, it may be that the cyclic structures must be vastly more stable than the linear structures to be observed under these conditions. Furthermore, in the molecular beam source used for this experiment, the graphite vapor is rapidly cooled by supersonic expansion, which may result in the "freezing-out" of high-energy structures produced in the initial vaporization. Recently, von Helden and colleagues reported an experimental (*26*) and theoretical (*27*) study of C_7^+ that illustrates these points. Both linear and cyclic isomers of C_7^+ were observed in mobility measurements. Ab initio calculations revealed that the cyclic structure should be approximately 20 kcal/mol more stable than the linear structure. A barrier to isomerization was also calculated to be about 50 kcal/mol. Thus, despite the large energy separation between the two isomers, a substantial number of linear structures form because of entropy and are subsequently frozen out because of the large barrier to isomerization. On the basis of these considerations, it seems likely that large linear carbon clusters play a major role in the chemistry of high-temperature, carbon-rich environments, despite the greater stability of the cyclic isomers.

REFERENCES AND NOTES

1. W. Weltner and R. Van Zee, *Chem. Rev.* **89**, 1713 (1989).
2. S. W. McElvany, M. M. Ross, N. S. Goroff, F. Diederich, *Science* **259**, 1594 (1993); G. von Helden, N. G. Gotts, M. T. Bowers, *Nature* **363**, 60 (1993), and references therein.
3. J. R. Chelikowsky, *Phys. Rev. Lett.* **67**, 2970 (1991).
4. K. S. Pitzer and E. Clementi, *J. Am. Chem. Soc.* **81**, 4477 (1959); R. Hoffman, *Tetrahedron* **22**, 521 (1966).
5. K. Raghavachari and J. S. Binkley, *J. Chem. Phys.* **87**, 2191 (1987).
6. D. E. Bernholdt, D. H. Magers, J. Bartlett, *ibid.* **89**, 3612 (1988); V. Parasuk and J. Almlöf, *ibid.* **91**, 1137 (1989); J. M. L. Martin, J. P. François, R. Gijbels, *ibid.* **93**, 8850 (1990); *ibid.* **94**, 3753 (1991); V. Parasuk and J. Almlöf, *ibid.*, p. 8172; J. Kurtz and L. Adamowicz, *Astrophys. J.* **370**, 784 (1991); Z. Slanina, J. Kurtz, L. Adamowicz, *Mol. Phys.* **76**, 387 (1992).
7. C. Liang, H. F. Schaefer III, *J. Chem. Phys.* **93**, 8844 (1990); J. D. Watts and R. J. Bartlett, *Chem. Phys. Lett.* **190**, 19 (1992).
8. J. M. L. Martin, J. P. François, R. Gijbels, J. Almlöf, *Chem. Phys. Lett.* **187**, 367 (1991).
9. J. Hutter, H. P. Lüthi, F. Diederich, *Research Report No. 93-107* (Interdisciplinary Project Center for Supercomputing, Swiss Federal Institute of Technology, Zurich, Switzerland, 1993).
10. D. Bakowies and W. Thiel, *J. Am. Chem. Soc.* **113**, 3704 (1991); M. Feyereisen, M. Gutowski, J. Simons, J. Almlöf, *J. Chem. Phys.* **96**, 2926 (1992); K. Raghavachari *et al.*, *Chem. Phys. Lett.* **214**, 357 (1993).
11. M. T. Bowers, P. R. Kemper, G. von Helden, P. A. M. van Koppen, *Science* **260**, 1446 (1993); G. von Helden, M. T. Hsu, N. G. Gotts, M. T. Bowers, *J. Phys. Chem.* **97**, 8182 (1993); G. von Helden, M. T. Hsu, N. G. Gotts, P. R. Kemper, M. T. Bowers, *Chem. Phys. Lett.* **204**, 15 (1993).
12. J. R. Heath and R. J. Saykally, in *On Clusters and Clustering*, P. J. Reynolds, Ed. (Elsevier Science, New York, 1993), pp. 7–21, and references therein.
13. K. W. H. Hinkle, J. J. Keady, P. F. Bernath, *Science* **241**, 1319 (1988); K. Kawaguchi, K. Matsumura, H. Kanamori, E. Hirota, *J. Chem. Phys.* **91**, 1953 (1989); F. J. Northrup, T. J. Sears, E. A. Rohlfing, *J. Mol. Spectrosc.* **145**, 74 (1991), and references therein; N. Moazzen-Ahmadi and A. R. W. McKellar, *J. Chem. Phys.* **98**, 7757 (1993).
14. N. Moazzen-Ahmadi, J. J. Thong, A. R. W. McKellar, *J. Chem. Phys.* **100**, 4033 (1994).
15. P. F. Bernath, K. H. Hinkle, J. J. Keady, *Science* **244**, 562 (1989); N. Moazzen-Ahmadi, S. D. Flatt, A. R. W. McKellar, *Chem. Phys. Lett.* **186**, 291 (1991).
16. H. J. Hwang *et al.*, *Mol. Phys.* **79**, 769 (1993).
17. A. Van Orden, H. J. Hwang, E. W. Kuo, R. J. Saykally, *J. Chem. Phys.* **98**, 6678 (1993).
18. D. Zajfman *et al.*, *Science* **258**, 1129 (1992), and references therein.
19. R. J. Van Zee, R. F. Ferrante, K. J. Zeringue, W. Weltner Jr., *J. Chem. Phys.* **86**, 5212 (1987); *ibid.* **88**, 3465 (1988).
20. D. W. Arnold, S. E. Bradforth, T. N. Kitsopoulos, D. M. Neumark, *ibid.* **95**, 8753 (1991).
21. M. B. Sowa and S. L. Anderson, *ibid.* **97**, 8164 (1992), and references therein.
22. G. von Helden, P. R. Kemper, N. G. Gotts, M. T. Bowers, *Science* **259**, 1300 (1993).
23. H. W. Kroto *et al.*, *Astrophys. J.* **314**, 352 (1987); J. R. Heath *et al.*, *J. Am. Chem. Soc.* **109**, 359 (1987).
24. Y. Achiba, C. Kittaka, T. Moriwaki, H. Shiromaru, *Z. Phys. D.* **19**, 427 (1991).
25. C. Q. Jiao *et al.*, *Rapid Commun. Mass Spectrom.* **7**, 404 (1993).
26. G. von Helden, N. G. Gotts, M. T. Bowers, *Chem. Phys. Lett.* **212**, 241 (1993).
27. G. von Helden, W. E. Palke, M. T. Bowers, *ibid.*, p. 247.
28. G. Guelachvili and K. N. Rao, *Handbook of Infrared Standards* (Academic Press, New York, 1986).
29. T.F.G. thanks the Max Kade Foundation, and A.V.O. thanks the NASA Graduate Student Researchers Program for support. Supported by the NASA Astrophysics Program under grant no. NAGW-2991 and the NASA Exobiology Program under grant no. NAGW-2763.

25 March 1994; accepted 9 June 1994

Direct Spectroscopic Detection of a Zwitterionic Excited State

Daniel S. Engebretson, Jeffrey M. Zaleski, George E. Leroi, Daniel G. Nocera*

Two electrons in two weakly coupled orbitals give rise to two states (diradical) with electrons residing in separate orbitals and two states (zwitterionic) with both electrons paired in one orbital or the other. This two-electron, two-orbital state manifold has eluded experimental confirmation because the zwitterionic states have been difficult to locate. Two-photon excitation of fluorescence from $Mo_2Cl_4(PMe_3)_4$ (D_{2d}) has been measured with linearly and circularly polarized light. From the polarization ratio and the energy of the observed transition, the 2^1A_1 ($\delta^*\delta^*$) excited state has been located and characterized. In conjunction with the one-photon allowed $^1B_2$ ($\delta\delta^*$) excited state, the zwitterionic state manifold for the quadruply bonded metal-metal class of compounds is thus established.

Two electrons in weakly coupled orbitals on two centers give rise to four states: two low-energy "diradical" states arising from one electron in each orbital with spins opposed (singlet) and parallel (triplet), respectively, and two higher energy "zwitterionic" singlet states derived from the antisymmetric and symmetric linear combinations, respectively, in which both electrons are paired in one orbital of either center. In this model, the singlet and triplet diradical states are energetically far removed from the ionic states, and the energy gaps within the diradical and zwitterionic states are small and equal. When the two orbitals are uncoupled, the diradical states are degenerate, as are the zwitterionic states. This two-electron, two-orbital manifold of states holds a central place in bonding descriptions. After their espial in the valence bond theory of Heitler and London (*1*), these states were invoked by Mulliken to describe ethylene upon twisting (*2*) and dihydrogen at long internuclear distances (stretched hydrogen) (*3*). They were subsequently recognized in Coulson and Fischer's treatment of dehydrogen by molecular orbital theory

---

Department of Chemistry and the LASER Laboratory, Michigan State University, East Lansing, MI 48824, USA.

*To whom correspondence should be addressed.

(*4*). The diradical states have been long established and have been at the foundation of the organic chemist's description of biradicals over the past two decades (*5*). However, the zwitterionic states are more elusive. The presence of zwitterionic states has been invoked to explain the isomerization and photocyclization of 1,3-dienes (*5*, *6*). Recently, solvent and substituent effects on the lifetimes of transient species resulting from the $\pi\pi^*$ excitation of alkenes have been rationalized on the basis of zwitterionic character in a twisted singlet excited state (*7*). Yet, the direct establishment of the zwitterionic states has heretofore not been achieved. We report the spectroscopic measurement of the zwitterionic excited state manifold resulting from the interaction of two electrons residing in adjacent and weakly coupled d_{xy} orbitals.

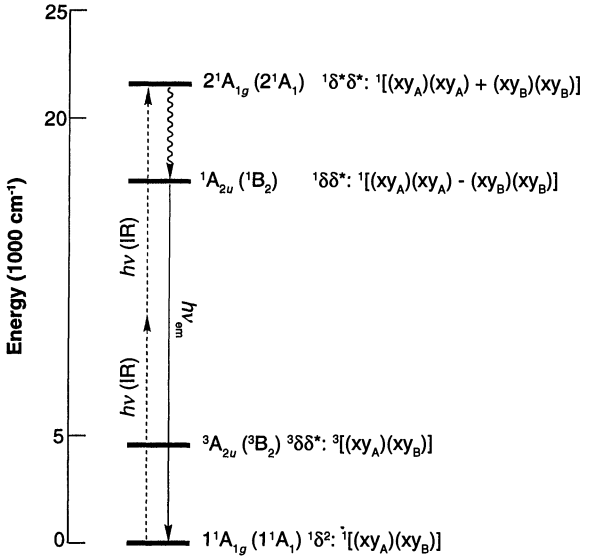

Fig. 1. Qualitative energy-level diagram for the δ/δ^* orbital manifold of $M\overset{4}{-}M$ complexes in accordance with a valence bond model. The state ordering is given for $M\overset{4}{-}M$ complexes in D_{4h} and D_{2d} symmetries (with the latter parenthetically offset); the d_{xy} orbitals on metal centers A and B are designated by (xy_A) and (xy_B), respectively. The two-photon experiment designed to detect the "zwitterionic" 2^1A_{1g} (A_1) excited state by laser-induced fluorescence is also summarized. The 2^1A_{1g} (A_1) state is pumped by two near-infrared photons [$h\nu$(IR), indicated by the dashed lines], followed by internal conversion to the highly emissive $^1A_{2u}$ (B_1) excited state. The red fluorescence $(h\nu_{em})$ from this state is detected.

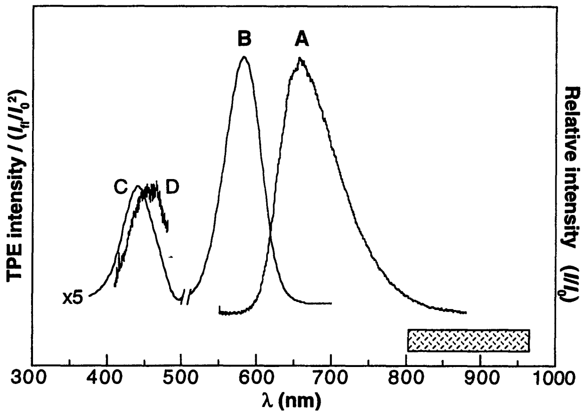

Fig. 2. Emission (**A**), absorption (**B** and **C**), and two-photon excitation (TPE) fluorescence (**D**) spectra from 10^{-3} M $Mo_2Cl_4(PMe_3)_4$ in 3-methylpentane at room temperature. Spectra A to C are described by the right ordinate axis, and spectrum D is described by the left ordinate axis. The absorption profile represented by B and C is discontinuous, with the ordinate axis of the latter magnified by a factor of 5: Spectrum C is magnified to highlight the energy difference of the one-electron $^1(\pi^4 \rightarrow \pi^3\delta^*)$ transition at 441 nm and the two-electron$^{-1}(\delta^2 \rightarrow {}^1\delta^{*2})$ transition at 455 nm. The two-photon fluorescence excitation spectrum is superposed at twice the laser excitation energy; the spectral region over which the incident dye-laser excitation was scanned is shown by the hatched box.

The overlap of the d_{z^2}, (d_{xz}, d_{yz}), and d_{xy} orbitals of two d^4 metals results in a $\sigma^2\pi^4\delta^2$ ground-state electronic configuration, which yields a quadruply bonded metal-metal $(M\overset{4}{-}M)$ complex (*8*). The lowest energy excited states of these complexes are therefore derived from the promotion of an electron from the δ to the δ^* orbital (*9*). Although a molecular orbital description approximates well the σ and π interactions, it does not provide a quantitative representation of the δ-bonding in $M\overset{4}{-}M$ complexes. The two electrons residing in the d_{xy} orbitals are weakly coupled, owing to the parallel disposition of the orbitals on each center to one another. Like twisted ethylene or stretched hydrogen, $M\overset{4}{-}M$ complexes with D_{4h} symmetry have been predicted with theoretical calculations (*10*) to have two diradical states of $1^1A_{1g}(\delta^2)$ and $^3A_{2u}$ $(^3\delta\delta^*)$ symmetry, energetically far removed from two zwitterionic states of $^1A_{2u}$ $(^1\delta\delta^*)$ and $2^1A_{1g}(^1\delta^{*2})$ symmetry (Fig. 1). The $^1A_{2u}$ excited state of $M\overset{4}{-}M$ complexes is highly luminescent, and the dipole-allowed $^1A_{2u} \leftarrow 1^1A_{1g}$ transition was assigned early in the study of the spectroscopy of these compounds (*8*, *9*). However, the zwitterionic nature of the $^1A_{2u}$ and 2^1A_{1g} excited states is not established in the absence of the latter state.

The 1^1A_{1g}–$^1A_{2u}$ energy gap is $K + \sqrt{K^2 + \Delta W^2}$, and the $^1A_{1g}$–2^1A_{1g} energy gap is $2\sqrt{K^2 + \Delta W^2}$, where K is the exchange integral and ΔW is the difference between the energies of the electron in singly occupied δ and δ^* orbitals, respectively (that is, $\Delta W = W_{\delta^*} - W_\delta$) (*11*). In the ionic limit where $K \gg \Delta W$, the difference in the energies of the zwitterionic states is, as expected, zero. Thus, the energetic disposition of 2^1A_{1g} relative to $^1A_{2u}$ is a direct measure of the ionicity of these zwitterionic excited states. With regard to this issue, the $2^1A_{1g} \leftarrow 1^1A_{1g}$ transition has escaped detection because it is inaccessible by conventional linear absorption spectroscopy, formally corresponding to the promotion of two electrons from the δ orbital to the δ^* orbital and therefore not allowed by one-photon, electric-dipole selection rules. However this two-electron transition is allowed in the two-photon spectrum (*12*). We have determined the energy of the two zwitterionic states by undertaking a comparative study of the one- and two-photon spectroscopy of $Mo_2Cl_4(PMe_3)_4$.

Figure 2 shows the conventional excitation and emission spectra of $Mo_2Cl_4(PMe_3)_4$ in 3-methylpentane at room temperature. The lowest energy absorption feature at 585 nm is attributable to the $\delta^2 \rightarrow \delta\delta^*$ $(^1B_2 \leftarrow 1^1A_1$ in D_{2d} symmetry) transition, and its excitation leads to bright red luminescence at a maximum wavelength (λ_{max}) of 673 nm (*13*, *14*). The bulky PMe_3 ligands lock the D_{2d} geometry of the complex, and the torsional distortion generally available to the $\delta\delta^*$ excited state is prevented (*15*). For this reason, the fluorescence of the $^1B_2(\delta\delta^*)$ excited state is prompt, intense, and a mirror image of the absorption profile (*13*). Detailed spectroscopic studies show no low-energy absorption features to the red of the $\delta^2 \rightarrow \delta\delta^*$ transition. Nevertheless, sample excitation with the output of a Nd:YAG-pumped dye laser between 800 and 970 nm leads to bright red luminescence, which when dispersed is revealed to be from the $\delta\delta^*$ excited state. The two-photon excitation (TPE) of fluorescence spectrum, obtained under linear polarization of the incident laser radiation, is superimposed in Fig. 2 (*16*). The fluorescence intensity varies with the square of the incident laser intensity (Figure 3A), as expected for a two-photon excitation process (*17*). A single peak at 455 nm is observed, which can be assigned with the aid of polarization information.

Figure 3B shows a point-by-point plot of the polarization ratio $(\Omega = I_{cir}/I_{lin})$ versus half the incident laser wavelength (*18*). The polarization ratio is constant and <1.0

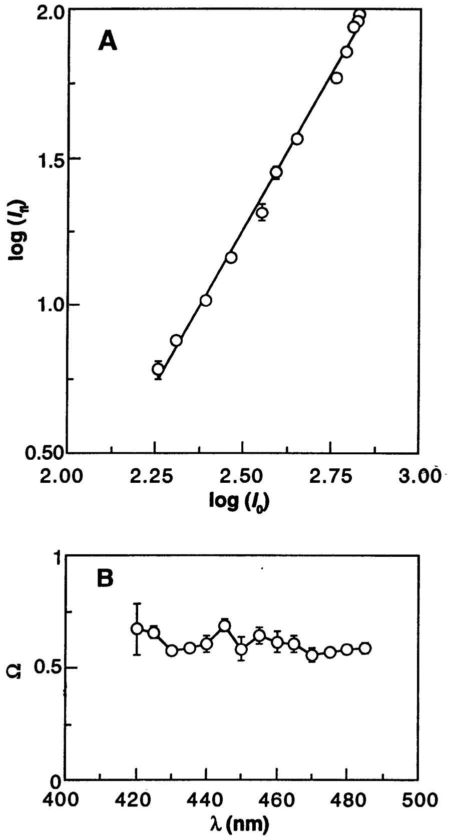

Fig. 3. (**A**) Representative plot of the two-photon fluorescence intensity versus the incident dye-laser intensity. These data were collected at an excitation wavelength of 860 nm in linear polarization; the slope is 2.05. For the other 35 measurements collected over the range of 800 to 970 nm (10-nm intervals) for both polarizations, similar results were obtained (slope = 2.00 ± 0.05). (**B**) Polarization ratio, Ω (I_{cir}/I_{lin}), plotted versus half the wavelength of the incident dye-laser radiation.

across the observed band, suggesting that the observed excitation envelope represents a single electronic state and is not a convolution of several bands. In the D_{2d} point group, the polarization ratio is <1 only for excited states of the same symmetry as the ground state (*19*), and therefore the two-photon excited state of $Mo_2Cl_4(PMe_3)_4$ must be of A_1 symmetry. Spectroscopic measurements of the lower and upper excited states of $Mo_2Cl_4(PMe_3)_4$ show that the second lowest energy singlet, one-photon excited state is $^1(\pi^4 \rightarrow \pi^3\delta^*)$, which lies to slightly higher energy (λ_{max} = 445 nm) than the observed two-photon transition (λ_{max} = 455 nm) (*13, 20*). Because two-electron transitions lie to higher energy than their one-electron counterparts, a two-photon transition at lower energy than $^1(\pi^4 \rightarrow \pi^3\delta^*)$ can only arise from the δ/δ^* manifold. The only reasonable assignment of the two-photon transition in Fig. 2 is $2^1A_1 \leftarrow 1^1A_1$ ($\delta^2 \rightarrow {}^1\delta^{*2}$). If similar Franck-Condon factors for the $\delta^2 \rightarrow {}^1\delta\delta^*$ and $\delta^2 \rightarrow {}^1\delta^{*2}$ transitions are assumed (*21*), then a 2^1A_1–$^1B_2$ energy gap of 4800 cm^{-1} is obtained for the zwitterionic excited-state manifold. This small energy gap relative to the $^1A_{2u} \leftarrow 1^1A_{1g}$ ($\delta^2 \rightarrow {}^1\delta\delta^*$) gap of 17,100 cm^{-1} establishes a very ionic, doubly excited state (*22*).

The two-photon spectroscopy result is in accord with several experiments involving $M\overset{4}{-}M$ complexes. The 2^1A_1–$^1B_2$ energy gap should be equivalent to the $^3B_2$–1^1A_1 energy gap of the diradical states, which has been experimentally measured for a series of twisted $M_2X_4(\overline{PP})_2$ (where $\overline{PP}$ is a bridging phosphine) complexes (*23*). The bridging ligands induce rotation about the metal-metal bond away from an eclipsed geometry [twist angle (χ) of 0°], where the δ bond is fully developed, to a nearly staggered geometry at χ = 45°, where the d_{xy} orbital overlap, and therefore the δ interaction, is annihilated. Although the $^3B_2$ excited state for $M\overset{4}{-}M$ complexes in eclipsed geometries is too high in energy to be populated at reasonable temperatures, a paramagnetic shift of the ^{31}P nuclear magnetic resonance signal arising from the $^3B_2$–1^1A_1 spin equilibrium can be measured for twisted $M_2X_4(\overline{PP})_2$ complexes. For twist angles from 17° to 64°, singlet-triplet energy separations of 1200 to 3000 cm^{-1} are observed; extrapolation to a torsional angle of 0° yields a diradical-state energy gap of 4840 cm^{-1} (*23*), in excellent agreement with theory (*24*) and the zwitterionic energy gap reported here. Moreover, because the zwitterionic transition places two electrons on a single metal center, the excited state is subject to instantaneous polarization due to perturbations by solvent. Picosecond time-resolved emission spectroscopy reveals that the temporal evolution of the emission from the $^1B_2$ state occurs on the time scale of the microscopic solvent relaxation (*25*). Presumably the Franck-Condon transition produces the $^1\delta\delta^*$ excited state with a solvent configuration appropriate for the apolar ground state. The system is stabilized as solvent moves to accommodate the instantaneously produced dipole. Hence, the emission spectrum evolves to its steady-state profile on the time scale of solvent motion.

The existence of zwitterionic states is well established in solid-state chemistry and physics. Indeed, the competition of one- and two-electron interaction energies has been invoked in the Hubbard model (*26*) to describe correlated electron motion in solids. Why then have these states not been directly observed in the system for which they were originally proposed, the chemical bond? The weak coupling characteristic of the zwitterionic states has only transitory existence during the stretching of bonds preceding dissociation or the twisting of bonds in isomerization. However, in the case of the $M\overset{4}{-}M$ systems, the weak coupling of parallel d_{xy} orbitals is maintained by the σ and π bond framework of the multiple metal-metal bond, and orbital orientation is locked by the ancillary ligands.

Finally, beyond its importance in models for chemical bonding, the zwitterionic excited-state manifold has important ramifications on chemical reactivity owing to the pairing of two electrons on one center and two holes on an adjacent one. This species is predisposed to multielectron reactivity and explains the photochemistry of $M\overset{4}{-}M$ complexes (*27*). More generally, zwitterionic states may prove to be critical intermediates in strategies to effect multielectron transformations in biology and chemistry.

REFERENCES AND NOTES

1. W. Heitler and F. London, *Z. Phys.* **44**, 455 (1927).
2. R. S. Mulliken, *Phys. Rev.* **41**, 751 (1932).
3. ——, *ibid.* **46**, 549 (1934); *ibid.* **50**, 1017, 1028 (1936); *ibid.* **51**, 315 (1937).
4. C. A. Coulson and I. Fischer, *Philos. Mag.* **40**, 386 (1949).
5. L. Salem and C. Rowland, *Angew. Chem. Int. Ed. Engl.* **11**, 92 (1972); J. Michl, *J. Mol. Photochem.* **4**, 243, 257 (1972); W. G. Dauben, L. Salem, N. J. Turro, *Acc. Chem. Res.* **8**, 41 (1975); W. T. Borden, *Diradicals* (Wiley, New York, 1982).
6. W. G. Dauben and J. S. Ritscher, *J. Am. Chem. Soc.* **92**, 2925 (1970); J. A. Marshall, *Science* **170**, 137 (1970); C. E. Wulfman and S. Kumei, *ibid.* **172**, 1061 (1971); W. G. Dauben, M. S. Kellogg, J. I. Seeman, N. D. Vietmeyer, P. H. Wendschuh, *Pure Appl. Chem.* **33**, 197 (1973); T. Tezuka *et al.*, *J. Am. Chem. Soc.* **103**, 1367 (1981); M. E. Squillacote and T. C. Semple, *ibid.* **109**, 892 (1987); V. Bonačić-Koutecký, J. Koutecký, J. Michl, *Angew. Chem. Int. Ed. Engl.* **26**, 170 (1987).
7. C. L. Schilling and E. F. Hilinski, *J. Am. Chem. Soc.* **110**, 2296 (1988); J. Morais, J. Ma, M. B. Zimmt, *J. Phys. Chem.* **95**, 3885 (1991); J. Ma and M. B. Zimmt, *J. Am. Chem. Soc.* **114**, 9723 (1992).
8. F. A. Cotton and R. A. Walton, *Multiple Bonds Between Metal Atoms* (Clarendon Press, Oxford, ed. 2, 1993).
9. W. C. Trogler and H. B. Gray, *Acc. Chem. Res.* **11**, 232 (1978).
10. P. J. Hay, *J. Am. Chem. Soc.* **104**, 7007 (1982).
11. M. D. Hopkins, H. B. Gray, V. M. Miskowski, *Polyhedron* **6**, 705 (1987).
12. W. M. McClain and R. A. Harris, in *Excited States*, E. C. Lim, Ed. (Academic Press, New York, 1977), vol. III, chap. 1.
13. M. D. Hopkins and H. B. Gray, *J. Am. Chem. Soc.* **106**, 2468 (1984).
14. V. M. Miskowski, H. B. Gray, M. D. Hopkins, *Inorg. Chem.* **31**, 2085 (1992).
15. J. R. Winkler, D. G. Nocera, T. L. Netzel, *J. Am. Chem. Soc.* **108**, 4451 (1986).
16. Fluorescence centered around 14,925 cm^{-1} from 10^{-3} M 3-methylpentane solution (Aldrich 99+% stored over activated 3A molecular sieves) of $Mo_2Cl_4(PMe_3)_4$ was induced by two-photon excitation from a Quanta Ray (Spectra Physics/Quanta Ray, Mountain View, CA) PDL-2 pulsed dye laser pumped by the 2^{nd} harmonic of a Quanta Ray DCR2 Nd:YAG laser. Five dye solutions with overlapping output ranges were used to provide excitation over the range of 10,310 to 12,500 cm^{-1}, with typical powers of 3 mJ per pulse. The intensity of the incident dye laser was monitored on each shot by an Si photodiode (Silicon Detector, Newberry Park, CA), and the output was stored in a Stanford Research Systems (Stanford, CA) SR250 boxcar integrator-averager. The fluo-

rescence was collected at right angles to the laser excitation beam and detected by a Hamamatsu R928 photomultiplier tube. Discrimination against scattered light was accomplished by a combination of filters (Corion LS-750-S) and a Spex (Edison, NJ) model 1680A monochromator. The dye-laser output was polarized by a Glan-Laser linear polarizer and passed through a set of three Fresnel rhombs before arriving at the sample. Two of the Fresnel rhombs are rotated together around the propagation axis of the excitation light, which allows the vector of the linearly polarized light to be rotated before it enters the third (stationary) rhomb. The dye laser wavelength, its intensity, and the fluorescence intensity measured by the photomultiplier were processed by a Compaq 386 microcomputer.

17. The transition probability for two-photon absorption from a single source, $W^{(2)}$, can be written as

$$W^{(2)} \propto I^2 \left| \sum_n \frac{\langle \psi_f | \mu | \psi_n \rangle \langle \psi_n | \mu | \psi_i \rangle}{\Delta E_{nI} - \hbar\omega_r} \right|^2$$

where I is the intensity of the incident laser beam, ψ_n is the virtual intermediate state, ψ_I and ψ_f are the initial and final states, respectively, μ is the electric dipole moment operator, ΔE_{nI} is the energy of the virtual state, $\hbar$ is Planck's constant divided by 2π, and ω_r is the frequency of the incident radiation. Thus, the transition probability is proportional to the square of the intensity of the incident laser beam. More generally, the transition probability for an n-photon process is proportional to I^n [S. H. Lin, Y. Fujimura, H. J. Neusser, E. W. Schlag, *Multiphoton Spectroscopy of Molecules* (Academic Press, Orlando, FL, 1984), chap. 4].

18. In one-photon spectroscopy, the absorption cross section, σ, for randomly oriented molecules is related to the transition dipole

$$\sigma \propto |\boldsymbol{\lambda} \cdot \mu_{fi}|^2$$

where $\boldsymbol{\lambda}$ is the unit polarization vector of the absorbed photon. Because $\lambda \cdot \lambda^* = 1$, there is no polarization information contained in the observed transition. In two-photon spectroscopy, however, the absorptivity is given by

$$\langle \delta \rangle = |\boldsymbol{\lambda} \cdot \mathbf{S}_{fi}^{ab} \cdot \boldsymbol{\kappa}|^2$$

where $\boldsymbol{\kappa}$ and $\boldsymbol{\lambda}$ are the polarization vectors of the two absorbed photons and $\mathbf{S}_{fi}^{ab}$ is the two-photon transition tensor. The polarization ratio, Ω, may be expressed in terms of the absorptivity in circular and linear polarizations, δ_{cir} and δ_{lin}, respectively

$$\Omega = \frac{\langle \delta_{cir} \rangle}{\langle \delta_{lin} \rangle}$$

If two photons of the same energy are used, then the polarization ratio is bounded by $0 \leq \Omega \leq 3/2$.

19. P. R. Monson and W. M. McClain, *J. Chem. Phys.* **53**, 29 (1970); W. M. McClain, *ibid.* **55**, 2789 (1971); M. A. Nasciemento, *Chem. Phys.* 74, 51 (1983).

20. M. D. Hopkins *et al.*, *J. Am. Chem. Soc.* **109**, 408 (1987); M. D. Hopkins, V. M. Miskowski, H. B. Gray, *ibid.* **110**, 1787 (1988).

21. Strictly speaking, this energy gap should be measured from the electronic origins of the two transitions, but the absence of vibrational fine structure in the two-photon spectrum precludes location of the 0–0 vibronic component.

22. From the effective overlap of 0.1 [as determined from the oscillator strength of the $\delta\delta^*$ transition (*11*)] and the spectroscopically determined ΔW and K from this work, the 34% ionic character of the ground state increases significantly to 68% in the zwitterionic excited state (J. F. Harrison, unpublished results).

23. M. D. Hopkins, T. C. Zietlow, V. M. Miskowski, H. B. Gray, *J. Am. Chem. Soc.* **107**, 510 (1985); F. A. Cotton, J. L. Eglin, B. Hong, C. A. James, *ibid.* **114**, 4915 (1992); F. A. Cotton, J. L. Eglin, B. Hong, C. A. James, *Inorg. Chem.* **32**, 2104 (1993).

24. F. A. Cotton and X. Feng, *J. Am. Chem. Soc.* **115**, 1074 (1993).

25. X. Zhang, M. Kozik, N. Sutin, J. R. Winkler, in *Electron Transfer in Inorganic, Organic, and Biological Systems*, J. R. Bolton, N. Mataga, G. McLendon, Eds. (American Chemical Society Advances in Chemistry Series no. 228, Washington, DC, 1991), pp. 247–264.

26. J. Hubbard, *Proc. R. Soc. London Ser. A* **276**, 238 (1963).

27. C. M. Partigianoni, I.-J. Chang, D. G. Nocera, *Coord. Chem. Rev.* **97**, 105 (1990); C. M. Partigianoni *et al.*, in *Mixed Valency Systems: Applications in Chemistry, Physics, and Biology*, K. Prassides, Ed. (NATO Advanced Study Institutes Series C no. 343, Kluwer Academic, Dordrecht, Netherlands, 1991), pp. 91–106; C. M. Partigianoni, C. Turró, T.-L. C. Hsu, I.-J. Chang, D. G. Nocera, in *Photosensitive Metal-Organic Systems*, C. Kutal and N. Serpone, Eds. (American Chemical Society Advances in Chemistry Series no. 238, Washington, DC, 1993), pp. 147–163; D. G. Nocera, in *The 30th Anniversary of the Quadruple Bond*, R. A. Walton, Ed. (Journal of Cluster Science no. 5, Plenum, New York, 1994), pp. 185–209.

28. Supported by the National Science Foundation under grants CHE-9100532 (D.G.N.) and CHE-9204136 (G.E.L.).

15 March 1994; accepted 3 June 1994

Antibody-Mediated Bacteriorhodopsin Orientation for Molecular Device Architectures

Koichi Koyama,* Naoto Yamaguchi, Tsutomu Miyasaka

A rational method for constructing highly oriented films of purple membrane (PM) has been established by using two kinds of bispecific antibodies with different antigen-binding sites, one binding to a specific side of bacteriorhodopsin and the other to a phospholipid hapten. A hapten monolayer deposited on a metal electrode was treated with a bispecific antibody solution and incubated with a PM suspension to produce a highly oriented PM film, as confirmed by electron microscopy in which an immunogold labeling technique was used. This antibody-mediated PM monolayer was then used in the construction of a light-sensing photoelectric device. A comparison of the two incorporated PM monolayers showed that highly efficient photocurrents were produced by the PM monolayer whose unidirectionally oriented cytoplasmic surface faces the electrode.

Bacteriorhodopsin (bR) is the sole protein found in the PM in *Halobacterium halobium*. Uniformly oriented bR molecules in PM perform unidirectional pumping of protons from the cytoplasm to the extracellular space during the photocycle, thereby forming an electrochemical gradient across the membrane. The three-dimensional structure and photocyclic reaction of bR have been well elucidated by Henderson and co-workers (*1*) and Khorana and co-workers (*2*).

The photocycle of bR and its rapid optical change (*3*) exhibit versatile photophysical functions in vitro; these functions can provide components that are critically important in the design of molecular electronic devices (*4*) and optical memories (*5*). We have verified that a PM-immobilized liquid-junction photocell exhibits differential electrical responsivity to light intensity, a function characteristic of vertebrate photoreceptors (*6*). One potential application for this responsivity is in the manufacture of an artificial retina that could detect and process optical information in a manner closely approximating certain visual functions (*7*).

In bR-based photoelectric devices, a truly integrated unidirectional—and thus highly efficient—electric response can be obtained only when the bR molecules have a nonrandom orientation. In this respect, efforts thus far to control the orientation of PM have included methods such as dispersion at the air-water interface, on charged membrane surfaces, in an electric field, and so forth (*8*). However, in most cases PM orientation is deduced on the basis of the direction and intensity of the photoelectric response of the PM monolayer after it has been incorporated into a device system. This sort of indirect approach frequently leads to conclusions that are confusing or contradictory (*8*).

The reason for this ambiguity is that no direct method has been devised that provides a precise means for controlling and determining the orientation of PM fragments. We have established an immunogold labeling technique that provides a highly accurate means of determining the ratio of orientation of PM sheets (*9*).

We describe a method to establish the perfect reorientation of bR through use of bispecific (BS) antibodies that simultaneously recognize both a phospholipid hapten and a specific side of the bR molecule. Our antibody technique is used to clarify the effect of bR orientation on bR-generated photoelectric events and to conclusively demonstrate the inherent advantages that the ability to precisely control PM orientation holds for the design of molecular devices.

N-(2,4-Dinitrophenyl)aminocaproyl phosphatidylethanolamine (DNP-cap PE,

---

Ashigara Research Laboratories, Fuji Photo Film Co. Ltd., Minamiashigara, Kanagawa, 250-01, Japan.

*To whom correspondence should be addressed.